Stromal beta-catenin activation impacts nephron progenitor differentiation in the developing kidney and may contribute to Wilms tumor

Keri A. Drake[1], Christopher P. Chaney[2], Amrita Das[3], Priti Roy[4], Callie S. Kwartler[5], Dinesh Rakheja[6], Thomas J. Carroll[2*]

[1]Division of Pediatric Nephrology, University of Texas Southwestern Medical Center, Dallas, TX

[2]Department of Molecular Biology and Internal Medicine, University of Texas Southwestern Medical Center, Dallas, TX

[3]Amgen, Inc. San Francisco, CA

[4]Department of Ophthalmology and Visual Sciences, Chicago, IL

[5]Division of Medical Genetics, Department of Internal Medicine, McGovern Medical School, University of Texas Health Science Center at Houston, Houston, TX

[6]Department of Pathology, University of Texas Southwestern Medical Center, Dallas, TX

*Corresponding author: Thomas.Carroll@UTSouthwestern.edu

Key words: beta-catenin, Wilms tumor, renal development, stroma, renal interstitium

SUMMARY STATEMENT

Stromal activation of beta-catenin drives gene expression changes similar to human Wilms tumor, suggesting that aberrant signaling from the stroma may contribute to tumorigenesis.

ABSTRACT

Wilms tumor (WT) morphologically resembles the embryonic kidney, consisting of blastema, epithelial, and stromal components, suggesting tumors arise from the dysregulation of normal development. Beta-catenin activation is observed in a significant proportion of WTs; however, much remains to be understood about how it contributes to tumorigenesis. While activating beta-catenin mutations are observed in both blastema and stromal components of WT, current models assume that activation in the blastemal lineage is causal. Paradoxically, studies performed in mice suggest that activation of beta-catenin in the nephrogenic lineage results in loss of nephron progenitor cell (NPC) renewal, a phenotype opposite to WT. Here, we show that activation of beta-catenin in the stromal lineage non-autonomously prevents the differentiation of NPCs. Comparisons of the transcriptomes of kidneys expressing an activated allele of beta-catenin in the stromal or nephron progenitor cells reveals that human WT more closely resembles the stromal-lineage mutants. These findings suggest that stromal beta-catenin activation results in histological and molecular features of human WT, providing insights into how alterations in the stromal microenvironment may play an active role in tumorigenesis.

INTRODUCTION

Wilms tumor, or nephroblastoma, is an embryonal tumor classically consisting of triphasic histology, with blastemal/nephron progenitor, epithelial, and stromal components thought to arise from disruptions in normal fetal nephrogenesis (Treger et al., 2019, Rivera and Haber, 2005, Hohenstein et al., 2015). During normal kidney development, nephron progenitor cells (NPCs) are maintained through renewing cell divisions. However, a subset of these cells simultaneously lose their progenitor cell identity and undergo mesenchymal-to-epithelial transition (MET) to form an immature tubule that will become a nephron, the functional unit of the kidney. A balance between self-renewal and differentiation is essential for generating kidneys with a sufficient number of nephrons necessary for function. This process is highly regulated and is known to rely on signals emanating from the epithelial cells of the ureteric bud as well as the surrounding stromal/interstitial signaling to the NPCs (Das et al., 2013, Fetting et al., 2014, Hum et al., 2014).

In a normal human kidney, the NPCs are exhausted prior to birth. However, in WT, blastemal cells/NPCs persist and continue proliferating well into the postnatal period. Still, much remains to be understood regarding the mechanism of this malignant transformation and resultant triphasic histology. Of particular relevance, the contribution of the stroma to Wilms tumorigenesis remains largely unknown. While the stroma/interstitium plays multiple roles in supporting normal tissue development and homeostasis, it has also been shown to contribute to tumor formation, progression, and metastasis in many cancers (Clark and Vignjevic, 2015, Li et al., 2007, Valkenburg et al., 2018). Tumor “stroma” refers to all components of the interstitium, including fibroblasts, immune cells, and vasculature (ie: endothelium and endothelial-associated mural cells) as well as the basement membrane and extracellular matrix (Bremnes et al., 2011). In this study, we will focus on the non-immune,

non-vascular, cellular components of the stroma, given that immature stroma/interstitial fibroblast cells abnormally persist and proliferate in WT.

Activating mutations in the gene encoding beta-catenin, CTNNB1, occur in about 15% of WTs (Li et al., 2004, Maiti et al., 2000). However, nuclear accumulation of beta-catenin is observed in up to 50% of tumors (Koesters et al., 2003), suggesting that aberrant activation of this pathway is critical in a significant proportion of WT. Beta-catenin is a component of the canonical Wnt signal transduction pathway. In the absence of a WNT ligand, beta-catenin is phosphorylated, sequestered in the cytoplasm, and tagged for degradation. However, in the presence of a WNT ligand, the cytoplasmic complex that phosphorylates beta-catenin dissociates, freeing beta-catenin to translocate into the nucleus and promote transcription. The mutations in the beta-catenin gene observed in WT render the protein insensitive to degradation, thus resulting in a constitutively stabilized form lacking regulation of its transcriptional activity.

In normal kidney development, Wnt/beta-catenin signaling regulates multiple aspects of nephrogenesis including nephron progenitor maintenance, mesenchymal-to-epithelial transition, ureteric bud progenitor renewal, and differentiation of the interstitium (Boivin and Bridgewater, 2018, Boivin et al., 2016, Park et al., 2007, Sarin et al., 2014, Marose et al., 2008, Karner et al., 2011, Ramalingam et al., 2018). Which of these processes is perturbed in WT is still unclear.

Nuclear expression of beta-catenin, as well as cells carrying CTNNB1 activating mutations, are observed among the different cell lineages of WT including blastemal, stromal, epithelial, and even heterologous components such as skeletal muscle (Corbin M, 2009, Duhme et al., 2019, Uschkereit et al., 2007). It has long been assumed that the causal mutation in WTs occurs in the blastemal component (Charles et al., 1998); however, recent studies performed in mice demonstrate that mutations in Wilms candidate genes (including

Lin28 and Wt1/Igf2) in the blastemal/nephron progenitor component alone are not sufficient to cause WT (Urbach et al., 2014, Huang et al., 2016). It is becoming increasingly apparent that the balance between nephron progenitor maintenance and differentiation is regulated by signals from the renal stroma, and we and others have shown that perturbations in stromal differentiation result in abnormally maintained NPCs reminiscent of nephrogenic rests in WTs (Das et al., 2013, Hum et al., 2014). Given the established roles of the stroma in tumor progression and its developmental role in regulating nephron differentiation, and that WT stroma harbors activating beta-catenin mutations, we decided to interrogate the role of the stroma in WT.

Here, we characterize mice carrying an activating mutation of beta-catenin specifically in the stromal progenitor population. We show that mutant kidneys form remnant epithelial structures surrounded by undifferentiated mesenchyme and spindle-shaped fibroblasts, similar to the histology of WT. Transcriptomes of mutant mouse kidneys with activating mutations in either the nephron progenitor lineage or the stromal lineage were compared to human WTs revealing that WT shares characteristic of the stromal-lineage mutants, more so than wild type developing kidney or NPC lineage mutants. Indeed, expression of Six2, Cited1, and Ncam, diagnostic markers of WT, is observed in the stromal lineage mutants and not the NPC lineage mutants. Finally, we show that activation of beta-catenin simultaneously in the nephron progenitor and stromal lineages (using dual Six2cre and Foxd1cre expression) results in severely disrupted kidney development with the formation of bone-like tissue, a phenotype that has been reported in human WT (Pritchard-Jones, 1997). These findings suggest that activation of beta-catenin in the stoma contributes to WT pathogenesis. Further understanding of the lineage-specific effects of beta-catenin activating mutations, as well as a more detailed analysis of the tumor stromal

microenvironment, may aid in unraveling the molecular and cellular mechanisms underlying WT.

RESULTS

Activating mutations of beta-catenin are found in both the stroma and NPCs of WT

Although it has long been known that WTs contain activating mutations in beta-catenin, the role of these mutations (drivers vs passenger) and the cell type of origin has been somewhat controversial. Several groups have shown that activating mutations in beta-catenin can be found in all cell types of WTs (Corbin M, 2009, Duhme et al., 2019, Uschkereit et al., 2007). To confirm these observations, we isolated stromal and blastemal cells using laser capture microdissection from three different WT samples carrying activating mutations of beta-catenin. In all three samples, the mutant allele was identified in both blastemal and stromal cellular components (representative data from one sample shown in Fig. 1). As the blastema and stroma arise from different cellular lineages in a normal kidney, and the two lineages appear to sort independently in early kidney development, the fact that the mutations are found in both cell populations within a tumor supports the claim that the mutagenic event occurred in a common precursor cell for both lineages (the intermediate mesoderm) and raises the possibility that activation in the stromal progenitor lineage contributes to the pathology of WT.

Activation of beta-catenin within different lineages of the metanephros severely perturbs renal development, with stromal activation demonstrating histological characteristics of Wilms tumor

Beta-catenin is ubiquitously expressed in the developing kidney. Through the use of various lineage restricted Cre lines and alleles of beta-catenin that can be activated or

inactivated by Cre, this factor has been shown to play a role in the balance of NPC maintenance and differentiation/mesenchymal-epithelial transition as well as development of interstitial cells and the ureteric bud progenitors (Boivin and Bridgewater, 2018, Boivin et al., 2016, Park et al., 2007, Sarin et al., 2014, Marose et al., 2008, Karner et al., 2011, Ramalingam et al., 2018, Yu et al., 2009). Although previous studies have characterized kidneys carrying activated alleles of beta-catenin ($Catnb^{ex3/+}$) within both the NPC and stromal lineages, we reanalyzed both mutants with a focus on their relationship to WT pathology. Six2Cre is active in the nephron progenitor cells, and Six2cre;$Catnb^{ex3/+}$ mutants lack developing nephrons and show premature loss of NPCs (Fig. 2, C). Lineage positive cells instead form aggregates of cells that persist throughout development that do not appear either mesenchymal or epithelial (Fig. 2, D and Supplemental Fig. 1).

Foxd1 is expressed in a population of mesenchymal cells in the cortex of the embryonic kidney and lineage tracing studies have shown that Foxd1-derived cells give rise to non-endothelial, non-immune stromal cells including pericytes, fibroblasts, mesangium, and vascular smooth muscle cells (Kobayashi et al., 2014). In comparison to activation with Six2Cre, activation of beta-catenin with Foxd1Cre (Foxd1cre;$Catnb^{ex3/+}$, from here on referred to as stromal or interstitial activation) results in abnormal maintenance of the NPC population, with delayed nephrogenesis (Fig 2, E). Gross morphologic examination revealed that stromal mutant kidneys were fused to the body wall. E18.5 kidneys showed a complete absence of mature nephrons (Fig. 2, F') with expanded interstitial cells surrounding undifferentiated NPCs and immature epithelia resembling renal vesicles or s-shaped bodies, grossly resembling the morphology of Wilms tumors. Lineage tracing of mutant kidneys derived from the two different Cre driver strains confirmed recombination in the expected nephron progenitor and stromal lineages, with the majority of lineage positive cells showing pathologically high levels of nuclear beta-catenin (Supplemental Fig. 1).

Activation of beta-catenin within the stromal lineage results in expanded nephron progenitor populations with delayed mesenchymal-to-epithelial transition

WTs are characterized by the expression of a number of genes normally associated with undifferentiated NPCs including Six2, Pax8 and Ncam. We thus sought to assess the expression of these markers in kidneys with activating mutations of beta-catenin in either lineage. Previous work suggests that activation of beta-catenin in the NPC lineage promotes differentiation, with decreased numbers of NPCs, an increased number of pre-tubular aggregate structures expressing Wnt4, Pax8, and Lhx1 and a blockade in MET/differentiation (Park et al., 2007). Re-analysis of these mutants shows that this "pre-tubular aggregate-like state" is transient, and by E15.5, NPCs lose Six2 expression as well as expression of Lhx1, Pax8, and Ncam (Fig. 3, G, H). Thus, at a molecular level, activation of beta-catenin within the NPC lineage does not lead to a WT-like phenotype nor does it lead to a maintenance of pre-tubular aggregate-like structures.

Next, we further examined the abnormally maintained NPCs in stromal mutant kidneys. In contrast to activation within the NPC lineage, E15.5 Foxd1cre;Catnb$^{ex3/+}$ kidneys maintain expression of Six2 and Ncam (Fig. 3 K, L and Fig. 4, H). However, expression of pre-tubular aggregate/differentiating NPC markers is abnormal, with some markers including C1qdc2 and Wnt4 showing expanded expression surrounding the NPCs while others, including Pax8 and Lhx1 are not expressed (Fig. 4, I-L, respectively). At E18.5, a small number of structures expressing Lhx1 are present (Fig. 4, N), corresponding to histologically identifiable renal vesicles and perhaps comma and S-shape bodies (Fig. 2, F). These findings suggest that stromal activation of beta-catenin not only non-autonomously blocks NPC differentiation, but also fundamentally alters the molecular state of these cells, demonstrating

that disruption of the normal stromal microenvironment significantly affects the differentiation of the neighboring NPC population.

Foxd1Cre mediated activation of beta-catenin disrupts stromal patterning

Previously, it has been shown that ablation of the stromal progenitor population results in abnormally maintained NPCs reminiscent of nephrogenic rests (Das et al., 2013). Foxd1cre;Catnb$^{ex3/+}$ kidneys show some hallmarks of these stroma-less kidneys, including abnormally expanded, Six2 expressing NPCs surrounding the UB (Fig. 3, K). Given these findings, we previously hypothesized that nephrogenic stromal cells produce a signal that promotes differentiation or blocks renewal of the NPCs. With this in mind, we examined the molecular phenotype of stromal cells upon activation of beta-catenin with Foxd1Cre. Foxd1cre;Catnb$^{ex3/+}$ kidneys show early loss of the stromal progenitor population as indicated by decreased expression of Foxd1, Netrin1 and Smoc2 (Fig. 5, G, H, and S, respectively). Instead, several genes normally expressed in the papillary stroma were precociously and ectopically expressed in the cortex, including Cpmx2, Sdc2, Dpp6, and Wnt5a, although Wnt4 papillary stroma expression was lost (Fig. 5, J, K, L, R and T respectively) (Shan et al., 2010). Mutant kidneys showed decreased expression of the cortico-medullary stromal markers Penk and Smoc2, as shown in Fig. 5, I and S, respectively. These findings suggest that activation of beta-catenin in the stromal progenitor cells may be leading to precocious and ectopic differentiation of a more papillary stromal cell type. Given that beta-catenin has previously been shown to be necessary for the development of the papillary stroma (Yu et al., 2009, Boivin and Bridgewater, 2018, Boivin et al., 2016), our findings suggest it is also sufficient.

Transcriptome profiling suggests human WT resembles mutant mouse kidneys with activation of beta-catenin specific to the stromal lineage

Previous transcriptional analyses of human WT suggests the up-regulation of numerous beta-catenin targets genes (Gadd et al., 2017, Li et al., 2004, Zirn et al., 2006). However, as beta-catenin is active in multiple lineages within the kidney and turns on unique targets in each lineage, we next sought to further characterize beta-catenin target genes up-regulated in human WT by investigating their expression in normal mouse kidneys as well as our lineage specific beta-catenin mutants. This was accomplished by performing RNA-Seq on both Six2cre;Catnb$^{ex3/+}$ and Foxd1cre;Catnb$^{ex3/+}$ mutant kidneys (Supplemental File 1). We next used BETA to integrate the differentially expressed genes from these mutant mouse models with beta-catenin CHIP-seq data (Supplemental File 2), thus generating a list of genes that are likely to be directly activated by beta-catenin in each lineage.

To identify genes that are likely to be mis-regulated in WT directly due to activation of beta-catenin, we then analyzed RNA-seq from WT samples in the TARGET database, comparing gene expression profiles of human Wilms tumors with and without CTNNB1 activating mutations and cross-referenced this data with the list of likely direct beta-catenin target genes from BETA (Supplemental File 3) and previously published targets. We next qualitatively compared this list to the lineage specific mutant mouse models to determine if one model more closely matched the expression pattern of WT with CTNNB1 activating mutations. There was no discernable alignment using this method or gene set enrichment analyses. In fact, somewhat unexpectedly, both mouse mutants showed up-regulation of several of the same WT enriched target genes. This is surprising given that many of these target genes, including Nkd1, Gap43, Axin2, Notum, MMP11, and Apcdd1 are normally expressed specifically in the papillary stroma of wildtype kidneys (Supplemental Fig. 2 and Fig. 6). Characterization of the expression of several of these genes in Six2cre;Catnb$^{ex3/+}$ and

Foxd1cre;Catnb$^{ex3/+}$ kidneys showed that all beta-catenin target genes assessed were precociously and ectopically expressed in both mutants (Fig 6). However, in the Foxd1cre mutants, target expression was observed in all Foxd1cre lineage positive stroma (rather than being restricted to the medullary interstitium) while in Six2cre mutants, expression was relatively normal in the papillary interstitium but was also observed ectopically in Six2cre derived cells.

We next developed a more comprehensive method to compare beta-catenin targets in human WT to our mutant mouse models. Given the considerable complexity and size of the TARGET data set, we utilized a deep learning classification technique. Using a trained neural network classifier, the expression profiles for 124 Wilms tumor samples were mapped to the expression data generated from kidneys of each of the three mouse genotypes (wild type, Six2cre;Catnb$^{ex3/+}$, and Foxd1cre;Catnb$^{ex3/+}$), resulting in a score ranging from 0 (no match) to 1.0 (representing a perfect match). As shown in Fig. 7, nearly all the human WT samples, including 6 tumors with known activating CTNNB1 mutations, showed almost exclusive mapping to the Foxd1cre;Catnb$^{ex3/+}$ transcriptome (scores ranging from 0.55 to 0.99), with only two samples showing an appreciable degree of similarity to wild type kidneys (scores of 0.28 and 0.44), and none of the samples mapping to the Six2cre;Catnb$^{ex3/+}$ expression profile (Supplemental File 4). This unbiased, quantitative approach, along with our histological studies, suggest that activation of beta-catenin in the NPC lineage does not appear to transcriptionally recapitulate Wilms tumor. Interestingly, despite human WT histologically resembling normal development, this analysis suggests that it is transcriptionally more similar to the mutant kidneys with stromal activation of beta-catenin than to normal, wild type embryonic kidney.

Activation of beta-catenin simultaneously within both the NPC and stromal lineages results in ectopic bone formation

Although our data suggest WT with activating mutations in beta-catenin are most similar at a molecular level to mouse kidneys with an activating mutation in the stromal lineage, neither Foxd1cre;Catnb$^{ex3/+}$ or Six2cre;Catnb$^{ex3/+}$ mutants precisely mimic WT. As it is likely that WTs acquire mutations in beta-catenin early in their history, we next sought to determine if activation of beta-catenin in both lineages was sufficient to lead to WT. We first sought to activate beta-catenin in cells that represented a common progenitor to both the stroma and NPCs utilizing T (brachyury)-creERT2. Using a Rosa-LSL-YFP lineage tracer, we observe recombination within the kidney when tamoxifen was administered to the TcreERT2;Catnb$^{ex3/+}$ embryos early in gestation at E7.5, 8.5 or 9.5; however, unexpectedly the kidneys appeared completely normal at E18.5 (Fig. 8) and at 4 months of age even though phenotypes outside the kidneys (such as curly tails) were visible (data not shown). Further analysis showed that lineage-positive cells within the kidney lacked detectable nuclear beta-catenin (Fig. 8, B). This was quite unexpected given the strong detectable nuclear beta-catenin staining observed in the Six2cre;Catnb$^{ex3/+}$ and Foxd1cre;Catnb$^{ex3/+}$ mutants (Fig. 8, C and D). This lack of nuclear beta-catenin in the TcreERT2 mutants suggests that early renal precursor cells expressing increased levels beta-catenin are preferentially selected against or subsequently down-regulate beta-catenin to allow continued development. Similar results were observed with another line driving Cre recombination in the intermediate mesoderm (Osr1CreERT2, data not shown).

To circumvent possible negative selection/cell competition, we simultaneously and uniformly activated beta-catenin in both the NPC and stromal lineages by creating Six2cre;Foxd1cre;Catnb$^{ex3/+}$ mutant kidneys. As shown in Fig. 2, Six2cre;Foxd1cre;Catnb$^{ex3/+}$ mutant kidneys show no distinguishable features of normal kidney development at E15.5,

with progenitor cells appearing to surround a primitive UB/nephric duct. Interestingly, by E18.5, these cells have a “bone-like” appearance, with histology showing a non-calcified, bone-like matrix and strong alkaline phosphatase staining within the lineage-positive cells (Fig. 9, A-C).

Although beta-catenin targets including Lef-1, a transcription factor involved in canonical Wnt/beta-catenin signaling that has also been shown to be a direct target of beta-catenin, are up-regulated in lineage-positive cells in all three mutant lines (Fig. 9, G-K), it is notable that the “bone-like” phenotype, which is observed in some Wilms tumors, is only observed in the Six2cre;Foxd1cre;Catnb$^{ex3/+}$ mutants. This observation clearly supports the hypothesis that activation of beta-catenin in the stromal lineage of WTs is not inert. We propose that activation of beta-catenin in the stroma contributes in multiple ways to WT pathology.

DISCUSSION

Wilms tumor, the most common type of kidney cancer in children, is thought to arise from transformed cells originating within the developing kidney. While WT1 and beta-catenin mutations were some of the first known pathways proposed in WT pathogenesis, advances in sequencing technology have revealed WT to be genetically heterogenous, with a number of different genetic perturbations commonly resulting in a preserved nephron progenitor state and/or interrupted normal development (Gadd et al., 2017, Treger et al., 2019).

Wnt/beta-catenin signaling plays a critical role in multiple aspects of normal kidney development and is up-regulated in a significant proportion of human WT. However, how beta-catenin drives tumorigenesis remains unclear. By examining the transcriptomic effects of beta-catenin activating mutations in multiple cell lineages of the developing kidney, we

have further defined how abnormal activation of this signaling pathway exerts both cell-type specific and lineage-independent effects in renal development. Although it has been proposed that activation of beta-catenin within the nephron progenitors or renal vesicles leads to tumor formation through inhibition of MET or activation of EMT, respectively, our findings suggest that activation of this gene within the mouse nephron progenitors and their derivatives does not lead to a Wilms tumor-like phenotype at the molecular level. However, activation of beta-catenin in the stromal progenitors results in impaired nephrogenesis, leading to nephrogenic rest-like structures that closely resemble human Wilms tumors at the transcriptional level. We show that Foxd1cre;Catnb$^{ex3/+}$ mutants maintain expression of Six2 and Ncam in the developing NPCs, similar to human WT blastema, whereas Six2cre;Catnb$^{ex3/+}$ mutants do not recapitulate this phenotype. Additionally, we show that the patterning of the renal interstitium is severely disrupted in Foxd1cre;Catnb$^{ex3/+}$ kidneys, with an early loss of Foxd1 progenitor cells and cortico-medullary stroma and a pronounced expansion of papillary stromal markers. While distinctions between cortical and medullary interstitial cells have been previously recognized, recent work has revealed a surprising degree of heterogeneity in the embryonic renal interstitium (England, 2020) suggesting that unique sub-populations of interstitial cells regulate adjacent cell types in normal kidney development. In support of this, inactivation of beta-catenin in the stromal progenitor population (using Foxd1Cre) blocks development of the papillary interstitium as well as adjacent epithelial cells of the loop of Henle (England, 2020, Yu et al., 2009). Conversely, we show here that activation of beta-catenin in the stromal progenitor population drives expression of papillary interstitial cells. We hypothesize that the abnormal interstitial patterning in the Foxd1cre;Catnb$^{ex3/+}$ kidneys disturbs the normal stromal microenvironment present in developing kidneys, leading to the altered gene expression and lack of differentiation in the NPC population. We hypothesize that a similar disruption to the stromal microenvironment contributes to Wilms tumorigenesis, as has been

suggested in numerous other tumors (Clark and Vignjevic, 2015, Mao et al., 2013, Bremnes et al., 2011, Valkenburg et al., 2018, Li et al., 2007).

It has long been assumed that driving mutations in Wilms tumor develop in the NPC/blastemal component. However, more recently, studies using laser microcapture techniques to analyze different components of human WT, including data from three patients in our study, demonstrate identical mutations in blastemal, stromal, and epithelial components consistent with beta-catenin mutations occurring in an early common precursor cell (Duhme et al., 2019, Uschkereit et al., 2007). Interestingly, our examination of mice with mosaic activation of beta-catenin in early metanephric precursor lineages utilizing TcreERT2 reveals that mutant cells were either selected against or down-regulated the forced expression of beta-catenin and underwent grossly normal development. In contrast, simultaneous activation of beta-catenin in the nephron progenitor and stromal lineages showed severely perturbed development with the formation of bone-like tissue. Interestingly, bone as well as other heterologous elements including cartilage and skeletal muscle have been reported in human WTs. Although these observations are consistent with a model in which activating mutations must occur in both NPC and stromal lineages (or a common progenitor for both), we cannot rule out the possibility that the triphasic morphology of WTs is due to aberrant tumor cell differentiation (through either multi-lineage potential or an ability to transdifferentiate) or that activating mutations in epithelial structures lead to EMT. Although we feel that the molecular phenotype of tumor stroma along with the histology of mouse mutants makes these possibilities unlikely (specifically, lineage traced NPC cells carrying an activated allele of beta-catenin do not take on a stromal appearance), it is clear that activation of beta-catenin alone is not sufficient to drive WT formation in mice and we cannot rule out contributions by other mutant genes.

Beta-catenin plays multiple, cell type specific roles during kidney development by activating different target genes (Pan et al., 2017). Surprisingly, stabilization of beta-catenin in either the stroma or the NPCs results in activation of the same stromal target genes. Previous studies have shown that different targets of beta-catenin are regulated in a dose-specific manner (Ramalingam et al., 2018). It is possible that the stromal targets represent genes activated by the highest levels of beta-catenin, independent of cell type. Another possibility is that the expression of co-regulators determines target gene expression. It is interesting to note that Lef-1 was over-expressed in all gain of function models (Six2cre, Foxd1cre and dual Six2cre;Foxd1cre) examined. The "stromal targets" of beta-catenin may actually be specific targets of a Lef-1/beta-catenin complex. These two hypotheses (which are not mutually exclusive) will need to be further explored.

Surprisingly, we observed no gross abnormalities in adulty kidneys upon mosaic activation of beta-catenin in the NPC, stromal or intermediate mesoderm lineages even though we did detect lineage positive cells. This is in contrast to a previous publication that found that activation of beta-catenin with Six2cre but not Foxd1cre resulted in tumor like structures in adult mice (Huang et al., 2016). We cannot explain the discrepancy; however, it is important to note that Huang et. al performed limited molecular characterization of their dysplastic tissues. Whether these lesions truly represent models of WT is still unclear. As we are unable to detect cells with nuclear beta-catenin in E18.5 or adult kidneys after mosaic activation of beta-catenin using standard immunofluorescence techniques, we hypothesize that under otherwise normal conditions strong beta-catenin activity either leads to precocious differentiation or is detrimental to cell survival (or both). In that case, additional mutations in genes affecting cell survival or differentiation may help to maintain these cells postnatally. Indeed, mutations in the WT1 gene, which affects NPC differentiation, as well as in p53, which impacts cell survival are frequently found in tumors with beta-catenin mutation (Huff,

2011, Maiti et al., 2000). It will be interesting to see if mutation of either of these interacts with beta-catenin activation, especially in the TcreERT2 context.

Given the heterogeneous nature of Wilms tumor, understanding the effects of beta-catenin activation in different cell lineages of the developing kidney in comparison to the molecular changes of human WT will aid in unraveling the pathogenesis of this embryonal tumor. While our data suggest that activation of beta-catenin in the stromal lineage of a mouse kidney is sufficient to alter the microenvironment in which nephrogenesis occurs and can lead to WT-like phenotypes, they certainly do not prove that this occurs in WTs as the lineage of the different cell types observed in WTs is still not known. Application of single cell transcriptomic techniques to Wilms' tumors of known genetic background will certainly be enlightening. No matter what, our findings provide additional insights into the genetic programs driven by beta-catenin in the developing kidney and suggest further studies are necessary to understand the role of stromal signaling in the development of Wilms tumor.

MATERIALS AND METHODS

Mouse models. Catnb$^{ex3/+}$, Six2cre, Foxd1cre, and TcreERT2 mouse lines *Mus musculus* were utilized as previously described (Harada et al., 1999, Kobayashi et al., 2014, Kobayashi et al., 2008, Imuta et al., 2013). All mice were bred on a mixed genetic background. For experimental assays described below, Catnb$^{ex3/ex3}$ females were crossed with male Cre-line mice, with day of plug counted as 0.5. Pregnant females were sacrificed at various gestational time points. Lineage tracing experiments were performed by crossing Rosa26YFP (JAX Stock #006148) or Rosa26Tomato (JAX Stock #007909) reporter mice with the above mouse lines. Mice with the desired genotype were randomly selected regardless of sex with Cre-negative littermates used as controls. Tamoxifen (Sigma, T5648) was administered by gavage at a dose of 2 mg per 40 g body weight. All animals were housed, maintained, and used

according to National Institutes of Health (NIH) and Institutional Animal Care and Use Committees (IACUC) approved protocols at the University of Texas Southwestern Medical Center (OLAW Assurance Number D16-00296).

Kidney sample preparation, immunostaining, and in-situ hybridization assays. Embryonic tissue was
fixed in 4% paraformaldehyde, embedded in paraffin, sectioned into 5 μm slices, and subjected to hematoxylin and eosin staining or immunofluorescence (IF). Slides for IF were immersed and boiled with either 10 mM sodium citrate or TE antigen retrieval buffer and blocked with a solution of 5% FBS/PBS for 1 hour at room temperature followed by the application of primary antibodies diluted in blocking solution. The following antibodies were used: GFP (Aves, Cat. GFP-1020, dilution 1:200), RFP (Rockland, Cat. 600-401-379, dilution 1:200), Ncam (Sigma, Cat. C9672, dilution 1:200), CK (DSHB, Cat. TROMA-I-s, dilution 1:50), Six2 (Proteintech, Cat. 11562-1-AP, dilution 1:200 and Abnova, Cat. H000110736-M01, dilution 1:200), beta-catenin (Sigma, Cat. C7207, dilution 1:200), Lhx1 (DSHB, Cat. 4F2-c, dilution 1:200), Pax8 (Proteintech, Cat. 10336-1-AP, dilution 1:200), and Lef-1 (Proteintech, Cat. 2230S, dilution 1:200). For in-situ hybridization assays, tissue was fixed with 4% paraformaldehyde, cryoprotected with 30% sucrose, embedded in OCT medium (TissueTek) sectioned into 10 μM slices, and rehydrated with PBS before being treated with 15 μg/mL proteinase K for 10 minutes and fixed in 4% PFA followed by an acetylation step. Slides were then washed and incubated with pre-hybridization buffer for 1 hour at room temperature before being hybridized with the specific probe overnight at 65°C. Slides were then washed in 0.2X SSC then transferred to NTT before blocking with 2% blocking solution (Roche) for at least 1 hour at room temperature. Slides were then incubated with Anti-Dig alkaline phosphatase conjugated antibody (Roche, 1:4000) overnight at 4°C.

The next day, slides were washed in NTT 3X and NTTML 3X before incubating with BM purple (Roche) for color reaction. After color reaction, slides were fixed with 4% PFA and mounted using Permount. E18.5 Six2cre;Foxd1cre;Catnb$^{ex3/+}$ bone-like tissue was fixed in 4% paraformaldehyde, decalcified with EDTA, sectioned into 5 μm slices, and subjected to hematoxylin and eosin staining, immunofluorescence, and alkaline phosphatase staining performed by our institutional histology core.

RNA Sequencing and analyses of gene expression data from the TARGET database. RNA sequencing was performed on mouse kidneys (E12.5 whole kidneys; N = 3 Cre-negative controls, 3 Foxd1cre;Catnb$^{ex3/+}$ mutants, and 3 Six2cre;Catnb$^{ex3/+}$ mutants). RNA was isolated from dissected kidneys stored in RNA later solution (Invitrogen, Cat. AM7020). RNA-Seq was performed using single end 75 bp with a minimum of 20 million reads per sample. Transcript abundance was estimated without aligning reads using Salmon (Patro et al., 2017) against an index of coding sequences from the Ensembl GRCm38 assembly. Transcript-level abundance was imported and count and offset matrices generated using the tximport R/Bioconductor package (Soneson et al., 2015). Differential expression analysis was performed using the DESeq2 R/Bioconductor package (Love et al., 2014). Wilms tumor expression data was downloaded from the TARGET database using the TCGAbiolinks R/Bioconductor package (Colaprico et al., 2016). A variance-stabilizing transformation implemented in the vst function of DESeq2 was applied prior to neural network processing.

To elucidate the relationship between activation of beta-catenin in either Six2 or Foxd1 lineage cells and Wilms tumor, we performed the following analysis. First, we used BETA (Wang et al., 2013) to integrate the results of RNA-sequencing of whole kidneys from Foxd1cre;Catnb$^{ex3/+}$, Six2cre;Catnb$^{ex3/+}$ and wild-type comparator mice with the previously

published beta-catenin ChIP-seq data (Park et al., 2012). This resulted a list of 2806 likely direct targets of beta-catenin. A neural network was then trained to classify the expression profiles of Foxd1cre;Catnb$^{ex3/+}$, Six2cre;Catnb$^{ex3/+}$ and wild-type kidneys based on the expression of these 2806 genes. Next, the expression profiles for 124 Wilms tumor samples curated in the TARGET database were mapped from human genes to mouse orthologues and then input to the neural network classifier. A sequential neural network with two hidden layers each containing 512 nodes was trained with the Adam optimizer using sparse categorical cross entropy loss using the TensorFlow platform ("TensorFlow White Papers | TensorFlow," n.d.). Five-fold cross validation was used during training. Classification scores ranging from 0 to 1.0 were assigned to each human Wilms tumor sample for each mouse genotype (wild type, Foxd1cre;Catnb$^{ex3/+}$, or Six2cre;Catnb$^{ex3/+}$). The scores sum to 1 for each tumor sample and so can be interpreted as a probability of identity. None of the samples showed significant similarity to Six2cre;Catnb$^{ex3/+}$ mutants.

Data Availability. RNA-seq data presented in this manuscript has been deposited into Gene Expression Omnibus; DOI is pending.

Statistical analysis. Data presented in figures are representative examples from one of at least three different

experiments on at least three different embryos/organs. No significant variability was noted in tissues of the same genotype; all animals with correct genotypes were included in the analysis. Bioinformatic statistics were carried about as described above; algorithms and software availability are provided in Supplemental File 5.

Footnotes:

- Competing interests: The authors declare no competing or financial interests.
- Author contributions: Experiments were designed by KD, CC, and TC. Experiments were performed by KD, CC, AD, PR, and CK. Data was interpreted by KD, CC, and TC. The paper was written by KD, CC, and TC.
- Funding: This study was supported by funding from the NIDDK to TC (RO1DK095057, RO1DK080004 and RO1DK080004). KD was partially supported by a UTSW SPORE CEP Award (P50CA196516) and a DOD KCRP Physician Research Award (W81XWH-19-1-0751) ARF was supported by F31DK122670. This work was supported by the UT Southwestern George O'Brien Kidney Research Core DK079328
- Data availability: RNA-seq data will be made publicly available through GEO; accession number is currently pending.
- Supplementary information

REFERENCES

BOIVIN, F. J. & BRIDGEWATER, D. 2018. beta-Catenin in stromal progenitors controls medullary stromal development. *Am J Physiol Renal Physiol,* 314**,** F1177-f1187.

BOIVIN, F. J., SARIN, S., DABAS, P., KAROLAK, M., OXBURGH, L. & BRIDGEWATER, D. 2016. Stromal beta-catenin overexpression contributes to the pathogenesis of renal dysplasia. *J Pathol,* 239**,** 174-85.

BREMNES, R. M., DØNNEM, T., AL-SAAD, S., AL-SHIBLI, K., ANDERSEN, S., SIRERA, R., CAMPS, C., MARINEZ, I. & BUSUND, L. T. 2011. The role of tumor stroma in cancer progression and prognosis: emphasis on carcinoma-associated fibroblasts and non-small cell lung cancer. *J Thorac Oncol,* 6**,** 209-17.

CHARLES, A. K., BROWN, K. W. & BERRY, P. J. 1998. Microdissecting the genetic events in nephrogenic rests and Wilms' tumor development. *Am J Pathol,* 153**,** 991-1000.

CLARK, A. G. & VIGNJEVIC, D. M. 2015. Modes of cancer cell invasion and the role of the microenvironment. *Curr Opin Cell Biol,* 36**,** 13-22.

COLAPRICO, A., SILVA, T. C., OLSEN, C., GAROFANO, L., CAVA, C., GAROLINI, D., SABEDOT, T. S., MALTA, T. M., PAGNOTTA, S. M., CASTIGLIONI, I., CECCARELLI, M., BONTEMPI, G. & NOUSHMEHR, H. 2016. TCGAbiolinks: an R/Bioconductor package for integrative analysis of TCGA data. *Nucleic Acids Res,* 44**,** e71.

CORBIN M, D. R. A., RICKMAN DS, BERREBI D, BOCCON-GIBOD L, COHEN-GOGO S, FABRE M, JAUBERT F, FAUSSILLON M, YILMAZ F, SARNACKI S, LANDMAN-PARKER J, PATTE C, SCHLEIERMACHER G, ANTIGNAC C,

JEANPIERRE C. 2009. WNT/beta-catenin pathway activation in Wilms tumors: a unifying mechanism with multiple entries? *Genes Chromosomes Cancer,* 48**,** 816-827.

DAS, A., TANIGAWA, S., KARNER, C. M., XIN, M., LUM, L., CHEN, C., OLSON, E. N., PERANTONI, A. O. & CARROLL, T. J. 2013. Stromal-epithelial crosstalk regulates kidney progenitor cell differentiation. *Nat Cell Biol,* 15**,** 1035-44.

DUHME, C., BUSCH, M., HEINE, E., DE TORRES, C., MORA, J. & ROYER-POKORA, B. 2019. WT1-Mutant Wilms Tumor Progression Is Associated With Diverting Clonal Mutations of CTNNB1. *J Pediatr Hematol Oncol*.

ENGLAND, A. R., CHANEY, C.P., DAS, A., PATEL, M., MALEWSAK, A., ARMENDARIZ, D., HON, G., STRAND, D., DRAKE, K.A., CARROLL, T.J. 2020. Characterization of interstitial heterogeneity in the developing kidney. *BioxRiv*.

FETTING, J. L., GUAY, J. A., KAROLAK, M. J., IOZZO, R. V., ADAMS, D. C., MARIDAS, D. E., BROWN, A. C. & OXBURGH, L. 2014. FOXD1 promotes nephron progenitor differentiation by repressing decorin in the embryonic kidney. *Development,* 141**,** 17-27.

GADD, S., HUFF, V., WALZ, A. L., OOMS, A., ARMSTRONG, A. E., GERHARD, D. S., SMITH, M. A., AUVIL, J. M. G., MEERZAMAN, D., CHEN, Q. R., HSU, C. H., YAN, C., NGUYEN, C., HU, Y., HERMIDA, L. C., DAVIDSEN, T., GESUWAN, P., MA, Y., ZONG, Z., MUNGALL, A. J., MOORE, R. A., MARRA, M. A., DOME, J. S., MULLIGHAN, C. G., MA, J., WHEELER, D. A., HAMPTON, O. A., ROSS, N., GASTIER-FOSTER, J. M., AROLD, S. T. & PERLMAN, E. J. 2017. A Children's Oncology Group and TARGET initiative exploring the genetic landscape of Wilms tumor. *Nat Genet,* 49**,** 1487-1494.

HARADA, N., TAMAI, Y., ISHIKAWA, T., SAUER, B., TAKAKU, K., OSHIMA, M. & TAKETO, M. M. 1999. Intestinal polyposis in mice with a dominant stable mutation of the beta-catenin gene. *Embo j,* 18**,** 5931-42.

HOEPPNER, L. H., SECRETO, F. J., RAZIDLO, D. F., WHITNEY, T. J. & WESTENDORF, J. J. 2011. Lef1DeltaN binds beta-catenin and increases osteoblast activity and trabecular bone mass. *J Biol Chem,* 286**,** 10950-9.

HOHENSTEIN, P., PRITCHARD-JONES, K. & CHARLTON, J. 2015. The yin and yang of kidney development and Wilms' tumors. *Genes Dev,* 29**,** 467-82.

HUANG, L., MOKKAPATI, S., HU, Q., RUTESHOUSER, E. C., HICKS, M. J. & HUFF, V. 2016. Nephron Progenitor But Not Stromal Progenitor Cells Give Rise to Wilms Tumors in Mouse Models with beta-Catenin Activation or Wt1 Ablation and Igf2 Upregulation. *Neoplasia,* 18**,** 71-81.

HUFF, V. 2011. Wilms' tumours: about tumour suppressor genes, an oncogene and a chameleon gene. *Nat Rev Cancer,* 11**,** 111-21.

HUM, S., RYMER, C., SCHAEFER, C., BUSHNELL, D. & SIMS-LUCAS, S. 2014. Ablation of the renal stroma defines its critical role in nephron progenitor and vasculature patterning. *PLoS One,* 9**,** e88400.

IMUTA, Y., KIYONARI, H., JANG, C. W., BEHRINGER, R. R. & SASAKI, H. 2013. Generation of knock-in mice that express nuclear enhanced green fluorescent protein and tamoxifen-inducible Cre recombinase in the notochord from Foxa2 and T loci. *Genesis,* 51**,** 210-8.

KARNER, C. M., DAS, A., MA, Z., SELF, M., CHEN, C., LUM, L., OLIVER, G. & CARROLL, T. J. 2011. Canonical Wnt9b signaling balances progenitor cell expansion and differentiation during kidney development. *Development,* 138**,** 1247-57.

KOBAYASHI, A., MUGFORD, J. W., KRAUTZBERGER, A. M., NAIMAN, N., LIAO, J. & MCMAHON, A. P. 2014. Identification of a multipotent self-renewing stromal progenitor population during mammalian kidney organogenesis. *Stem Cell Reports,* 3**,** 650-62.

KOBAYASHI, A., VALERIUS, M. T., MUGFORD, J. W., CARROLL, T. J., SELF, M., OLIVER, G. & MCMAHON, A. P. 2008. Six2 defines and regulates a multipotent self-renewing nephron progenitor population throughout mammalian kidney development. *Cell Stem Cell,* 3**,** 169-81.

KOESTERS, R., NIGGLI, F., VON KNEBEL DOEBERITZ, M. & STALLMACH, T. 2003. Nuclear accumulation of beta-catenin protein in Wilms' tumours. *J Pathol,* 199**,** 68-76.

LI, C. M., KIM, C. E., MARGOLIN, A. A., GUO, M., ZHU, J., MASON, J. M., HENSLE, T. W., MURTY, V. V., GRUNDY, P. E., FEARON, E. R., D'AGATI, V., LICHT, J. D. & TYCKO, B. 2004. CTNNB1 mutations and overexpression of Wnt/beta-catenin target genes in WT1-mutant Wilms' tumors. *Am J Pathol,* 165**,** 1943-53.

LI, H., FAN, X. & HOUGHTON, J. 2007. Tumor microenvironment: the role of the tumor stroma in cancer. *J Cell Biochem,* 101**,** 805-15.

LI, Z., XU, Z., DUAN, C., LIU, W., SUN, J. & HAN, B. 2018. Role of TCF/LEF Transcription Factors in Bone Development and Osteogenesis. *Int J Med Sci,* 15**,** 1415-1422.

LOVE, M. I., HUBER, W. & ANDERS, S. 2014. Moderated estimation of fold change and dispersion for RNA-seq data with DESeq2. *Genome Biol,* 15**,** 550.

MAITI, S., ALAM, R., AMOS, C. I. & HUFF, V. 2000. Frequent association of beta-catenin and WT1 mutations in Wilms tumors. *Cancer Res,* 60**,** 6288-92.

MAO, Y., KELLER, E. T., GARFIELD, D. H., SHEN, K. & WANG, J. 2013. Stromal cells in tumor microenvironment and breast cancer. *Cancer Metastasis Rev,* 32**,** 303-15.

MAROSE, T. D., MERKEL, C. E., MCMAHON, A. P. & CARROLL, T. J. 2008. Beta-catenin is necessary to keep cells of ureteric bud/Wolffian duct epithelium in a precursor state. *Dev Biol,* 314**,** 112-26.

PAN, X., KARNER, C. M. & CARROLL, T. J. 2017. Myc cooperates with β-catenin to drive gene expression in nephron progenitor cells. *Development,* 144**,** 4173-4182.

PARK, J. S., MA, W., O'BRIEN, L. L., CHUNG, E., GUO, J. J., CHENG, J. G., VALERIUS, M. T., MCMAHON, J. A., WONG, W. H. & MCMAHON, A. P. 2012. Six2 and Wnt regulate self-renewal and commitment of nephron progenitors through shared gene regulatory networks. *Dev Cell,* 23**,** 637-51.

PARK, J. S., VALERIUS, M. T. & MCMAHON, A. P. 2007. Wnt/beta-catenin signaling regulates nephron induction during mouse kidney development. *Development,* 134**,** 2533-9.

PATRO, R., DUGGAL, G., LOVE, M. I., IRIZARRY, R. A. & KINGSFORD, C. 2017. Salmon provides fast and bias-aware quantification of transcript expression. *Nat Methods,* 14**,** 417-419.

PRITCHARD-JONES, K. 1997. Malignant origin of the stromal component of Wilms' tumor. *J Natl Cancer Inst,* 89**,** 1089-1091.

RAMALINGAM, H., FESSLER, A. R., DAS, A., VALERIUS, M. T., BASTA, J., ROBBINS, L., BROWN, A. C., OXBURGH, L., MCMAHON, A. P., RAUCHMAN, M. & CARROLL, T. J. 2018. Disparate levels of beta-catenin activity determine nephron progenitor cell fate. *Dev Biol,* 440**,** 13-21.

RIVERA, M. N. & HABER, D. A. 2005. Wilms' tumour: connecting tumorigenesis and organ development in the kidney. *Nat Rev Cancer,* 5**,** 699-712.

SARIN, S., BOIVIN, F., LI, A., LIM, J., SVAJGER, B., ROSENBLUM, N. D. & BRIDGEWATER, D. 2014. beta-Catenin overexpression in the metanephric mesenchyme leads to renal dysplasia genesis via cell-autonomous and non-cell-autonomous mechanisms. *Am J Pathol,* 184**,** 1395-410.

SHAN, J., JOKELA, T., SKOVORODKIN, I. & VAINIO, S. 2010. Mapping of the fate of cell lineages generated from cells that express the Wnt4 gene by time-lapse during kidney development. *Differentiation,* 79**,** 57-64.

SONESON, C., LOVE, M. I. & ROBINSON, M. D. 2015. Differential analyses for RNA-seq: transcript-level estimates improve gene-level inferences. *F1000Res,* 4**,** 1521.

TREGER, T. D., CHOWDHURY, T., PRITCHARD-JONES, K. & BEHJATI, S. 2019. The genetic changes of Wilms tumour. *Nat Rev Nephrol,* 15**,** 240-251.

URBACH, A., YERMALOVICH, A., ZHANG, J., SPINA, C. S., ZHU, H., PEREZ-ATAYDE, A. R., SHUKRUN, R., CHARLTON, J., SEBIRE, N., MIFSUD, W., DEKEL, B., PRITCHARD-JONES, K. & DALEY, G. Q. 2014. Lin28 sustains early renal progenitors and induces Wilms tumor. *Genes Dev,* 28**,** 971-82.

USCHKEREIT, C., PEREZ, N., DE TORRES, C., KUFF, M., MORA, J. & ROYER-POKORA, B. 2007. Different CTNNB1 mutations as molecular genetic proof for the independent origin of four Wilms tumours in a patient with a novel germ line WT1 mutation. *J Med Genet,* 44**,** 393-6.

VALKENBURG, K. C., DE GROOT, A. E. & PIENTA, K. J. 2018. Targeting the tumour stroma to improve cancer therapy. *Nat Rev Clin Oncol,* 15**,** 366-381.

WANG, S., SUN, H., MA, J., ZANG, C., WANG, C., WANG, J., TANG, Q., MEYER, C. A., ZHANG, Y. & LIU, X. S. 2013. Target analysis by integration of transcriptome and ChIP-seq data with BETA. *Nat Protoc,* 8**,** 2502-15.

YU, J., CARROLL, T. J., RAJAGOPAL, J., KOBAYASHI, A., REN, Q. & MCMAHON, A. P. 2009. A Wnt7b-dependent pathway regulates the orientation of epithelial cell division and establishes the cortico-medullary axis of the mammalian kidney. *Development*, 136**,** 161-71.

ZIRN, B., SAMANS, B., WITTMANN, S., PIETSCH, T., LEUSCHNER, I., GRAF, N. & GESSLER, M. 2006. Target genes of the WNT/beta-catenin pathway in Wilms tumors. *Genes Chromosomes Cancer*, 45**,** 565-74.

Figures

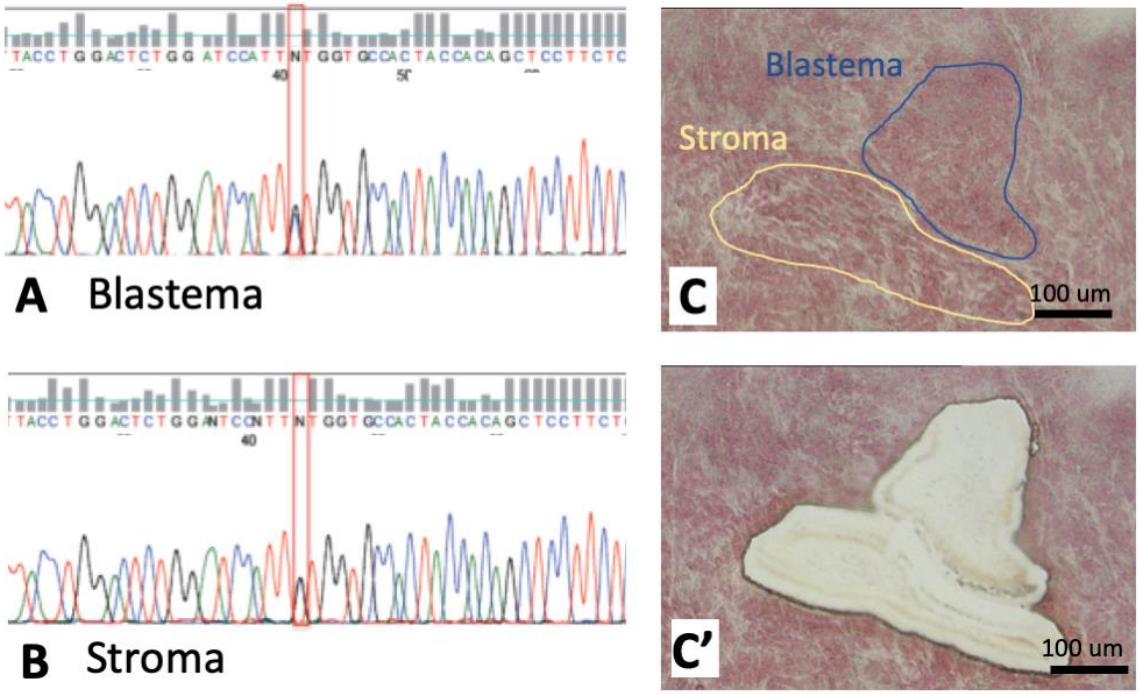

Figure 1. Both blastemal and stromal components of human Wilms tumor carry CTNNB1 activating mutations. Sequence reads of DNA extracted from blastema (A) and stroma/interstium (B) isolated with laser microcapture dissection (C) are shown from a representative tumor, demonstrating that both cell populations carry the same CTNNB1 point mutation. Two additional tumors analyzed show the same frame shift in the second tumor and the same in/del in the third (data not shown). Scale bar = 100 um.

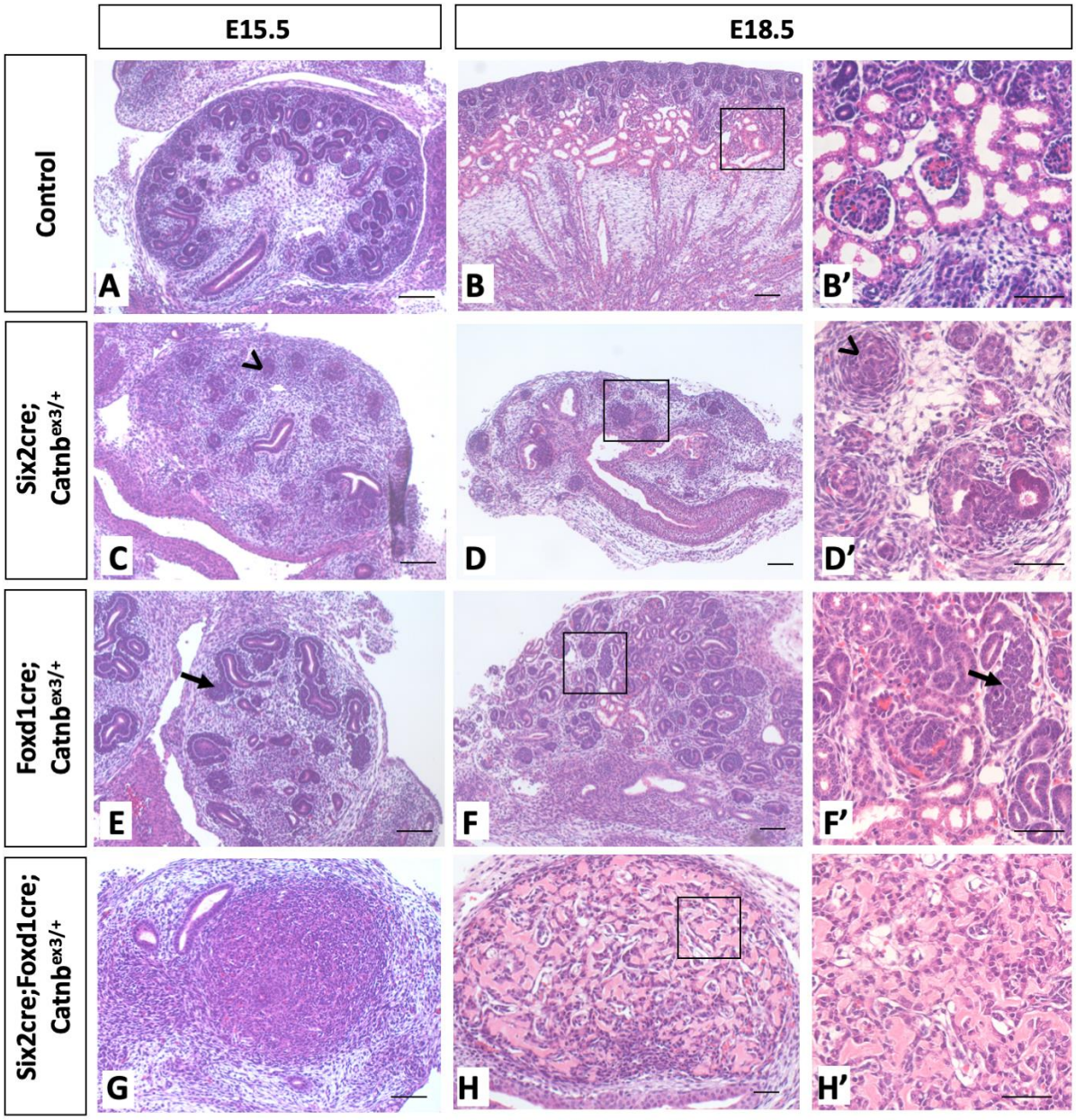

Figure 2. Activation of beta-catenin in different lineages of the developing kidney severely perturbs nephrogenesis, with stromal activation resulting in abnormal maintenance of NPCs and disrupted MET. Foxd1cre;Catnb$^{ex3/+}$ kidneys show abnormally maintained NPCs with a lack differentiating structures at E15.5 (E, arrow). By E18.5, some NPCs are induced and undergo nephrogenesis, but regions of abnormally maintained NPCs remain in the developing kidney (F' arrow). Conversely, Six2cre;Catnb$^{ex3/+}$ kidneys show

early loss of NPCs and lack of MET (C, D). Six2cre;Foxd1cre;Catnb$^{ex3/+}$ kidneys show little resemblance to the developing metanephros and form bone-like tissue later in development (H, K'). Scale bar = 100 um; N = 3 for each timepoint/genotype.

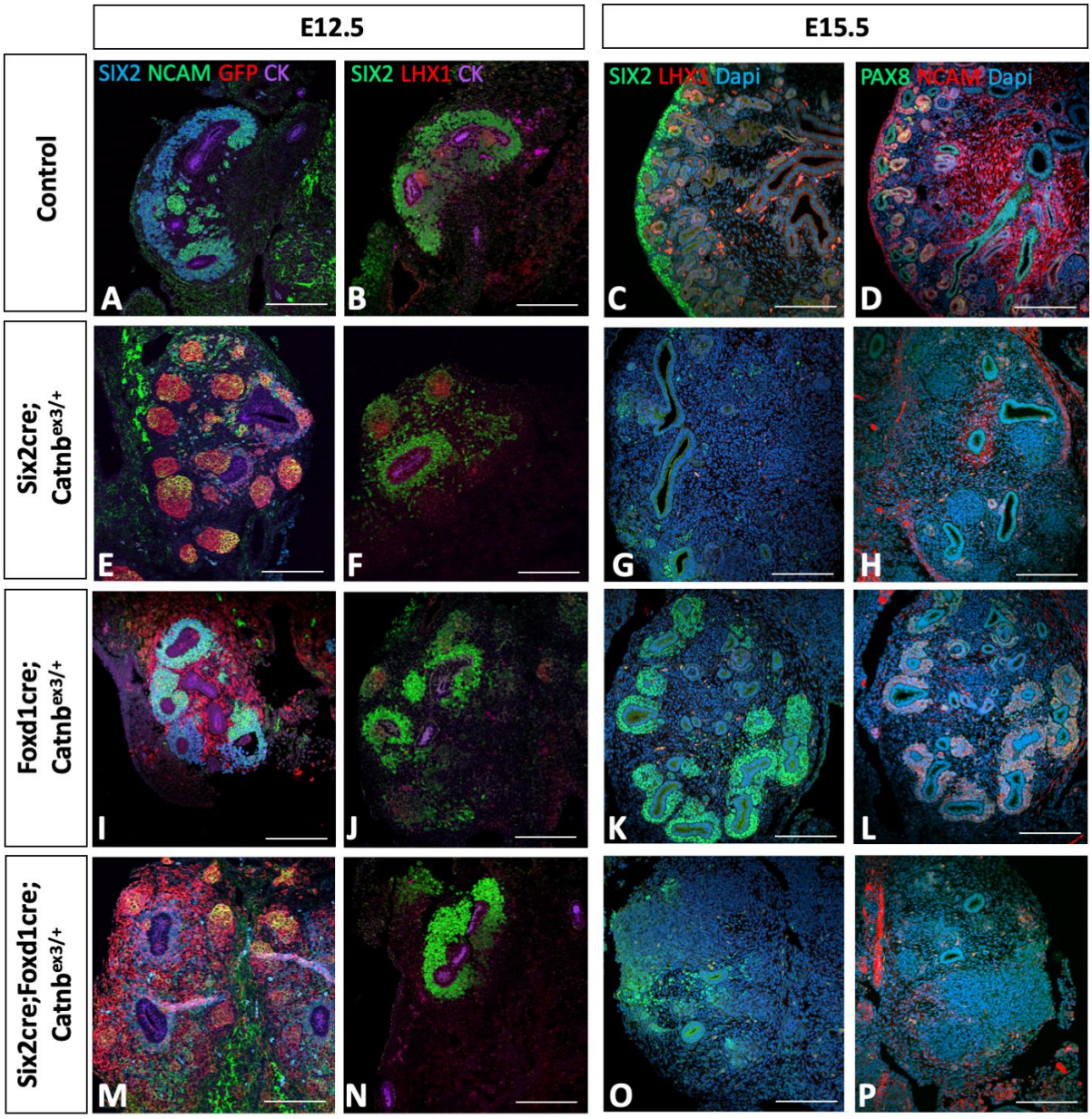

Figure 3. Beta-catenin activation within the nephron progenitor lineage results in premature loss of the nephron progenitor/blastemal cells, while the opposite phenotype is observed in beta-catenin activation within the stroma. Six2cre;Catnb$^{ex3/+}$ mutant kidneys show early loss of Six2 positive NPCs with transient expression of Ncam (E) and Lhx1(F) consistent with a "pre-tubular aggregate (PTA) like state" as previously published. However, by E15.5, these cells no longer express PTA or renal vesicle markers including

Lhx1, Pax8, and Ncam (G, H). Comparatively, Foxd1cre;Catnb$^{ex3/+}$ mutant kidneys maintain Six2 and Ncam expression (K, L). At E15.5, Six2cre;Foxd1cre;Catnb$^{ex3/+}$ mutants resemble Six2cre;Catnb$^{ex3/+}$ mutants, with loss of Six2 positive NPCs that lack Ncam expression (O, P). Scale bar = 100 um; N = 3 for each timepoint/genotype.

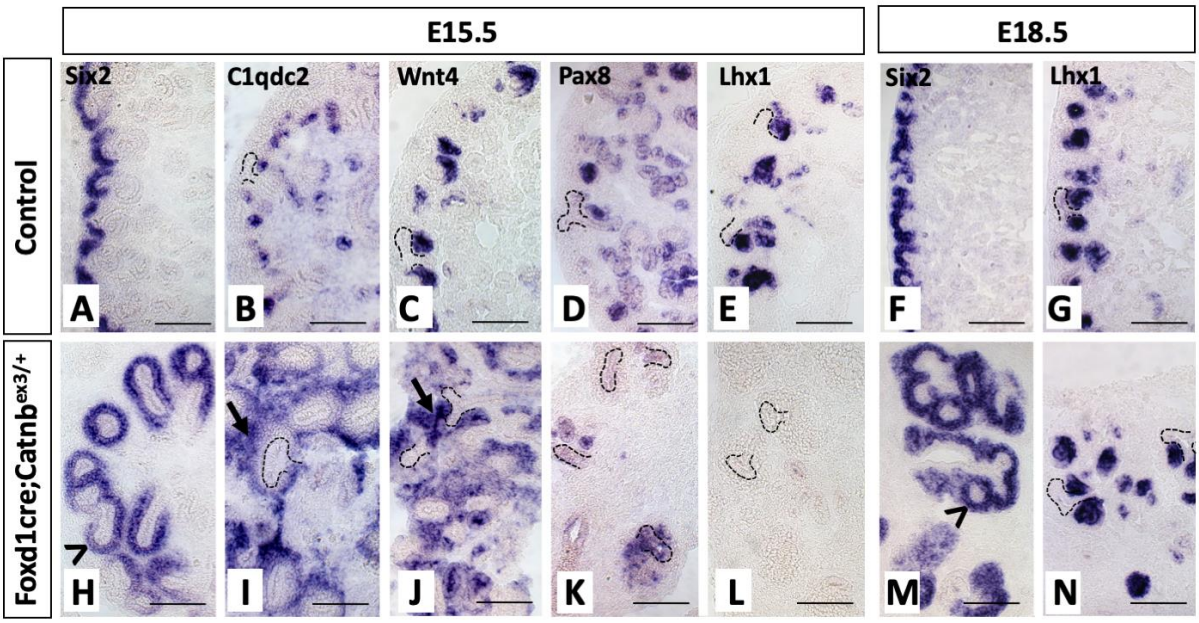

Figure 4. Beta-catenin activation in stromal lineage results in expanded nephron progenitor cells with delayed MET. NPCs of Foxd1cre;Catnb$^{ex3/+}$ mutant kidneys show abnormal expansion at E15.5 expressing both markers of both self-renewal (H - Six 2) and early commitment to differentiation/MET (I - C1qdc2, J – Wnt4) but lack expression of other MET markers (K - Pax8 and L - Lhx1). By E18.5, however, Lhx1 positive structures are present (N) corresponding to histologically identifiable comma and S-shape like bodies on H&E. Scale bar = 100 um; N = 3 for each timepoint/genotype.

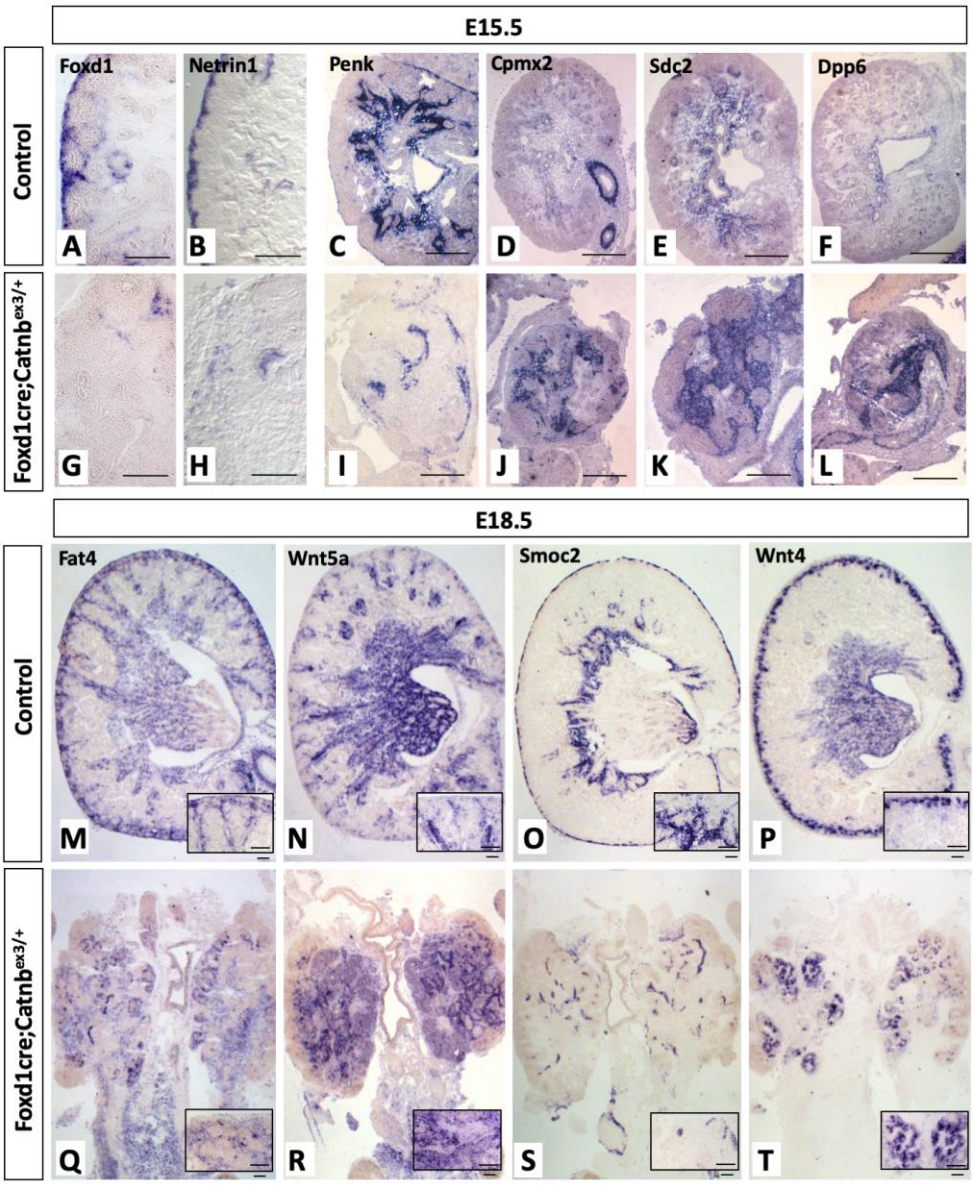

Figure 5. Beta-catenin activation in stromal lineage disrupts normal interstitial patterning. Foxd1cre;Catnb$^{ex3/+}$ mutants show early loss of the Foxd1+ stromal progenitor population (G) and nephrogenic interstitial markers Netrin1 (H) and Smoc2 (S). Medullary stromal markers appear ectopically expressed in the cortex, including Cpmx2 (J), Sdc2 (K), Dpp6 (L), and Wnt5a (R) with loss of expression of the corticomedullary markers, Penk (I) and Smoc2 (S). Scale bar = 100 um; N = 3 for each timepoint/genotype.

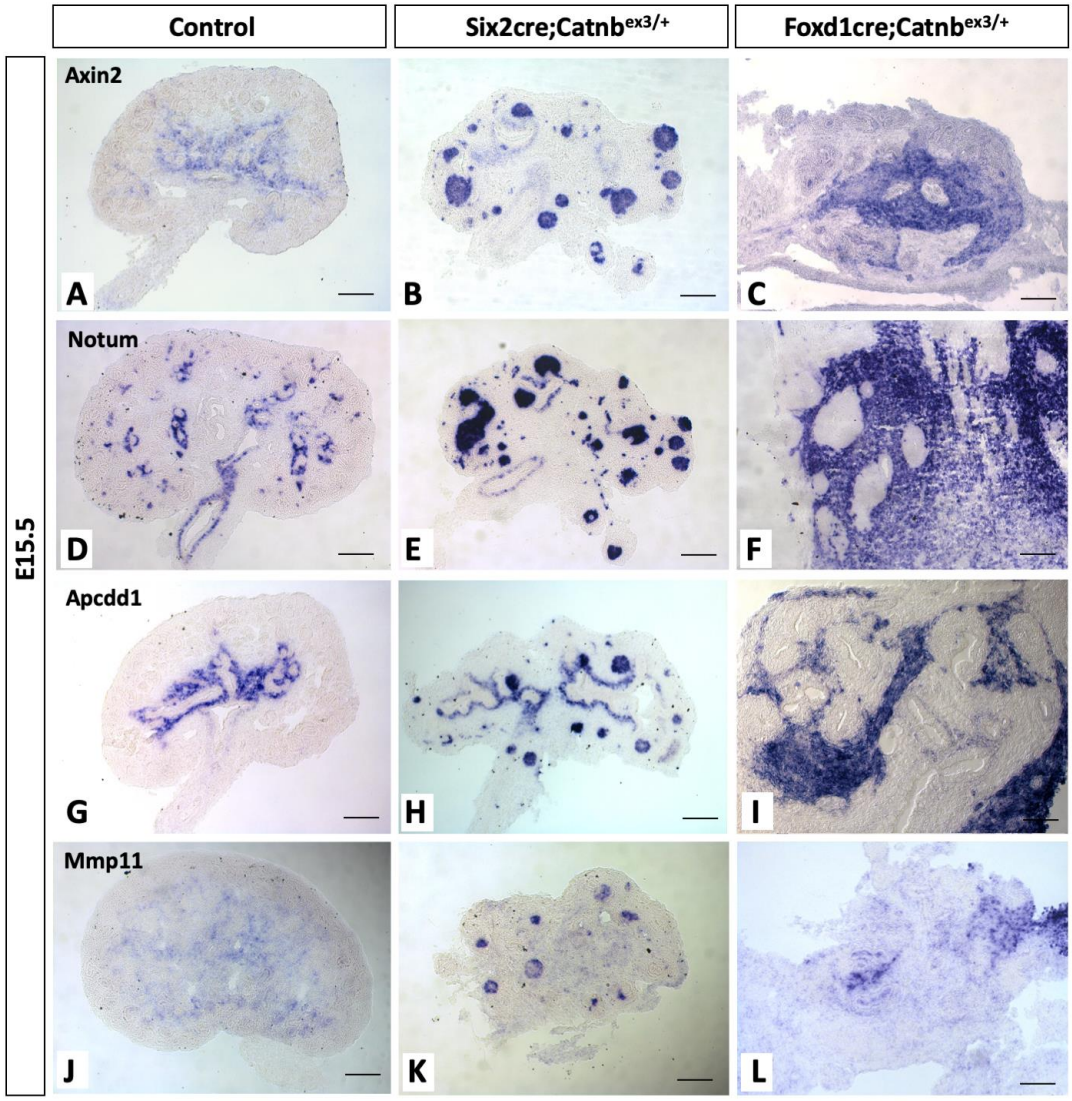

Figure 6. Beta-catenin activation in either the NPC or stromal lineages drives the expression of genes normally localized to the developing renal interstitium.

Foxd1cre;Catnb$^{ex3/+}$ mutants show up-regulation of multiple stromal markers as expected given the known role of beta-catenin in the development of the medullary interstitium. However, these same target genes are up strongly up-regulated in Six2cre;Catnb$^{ex3/+}$ cells, somewhat unexpectedly given that these cells originate from a separate lineage where this transcriptional program is not active during normal development. Scale bar = 100 um; N = 3 for each timepoint/genotype

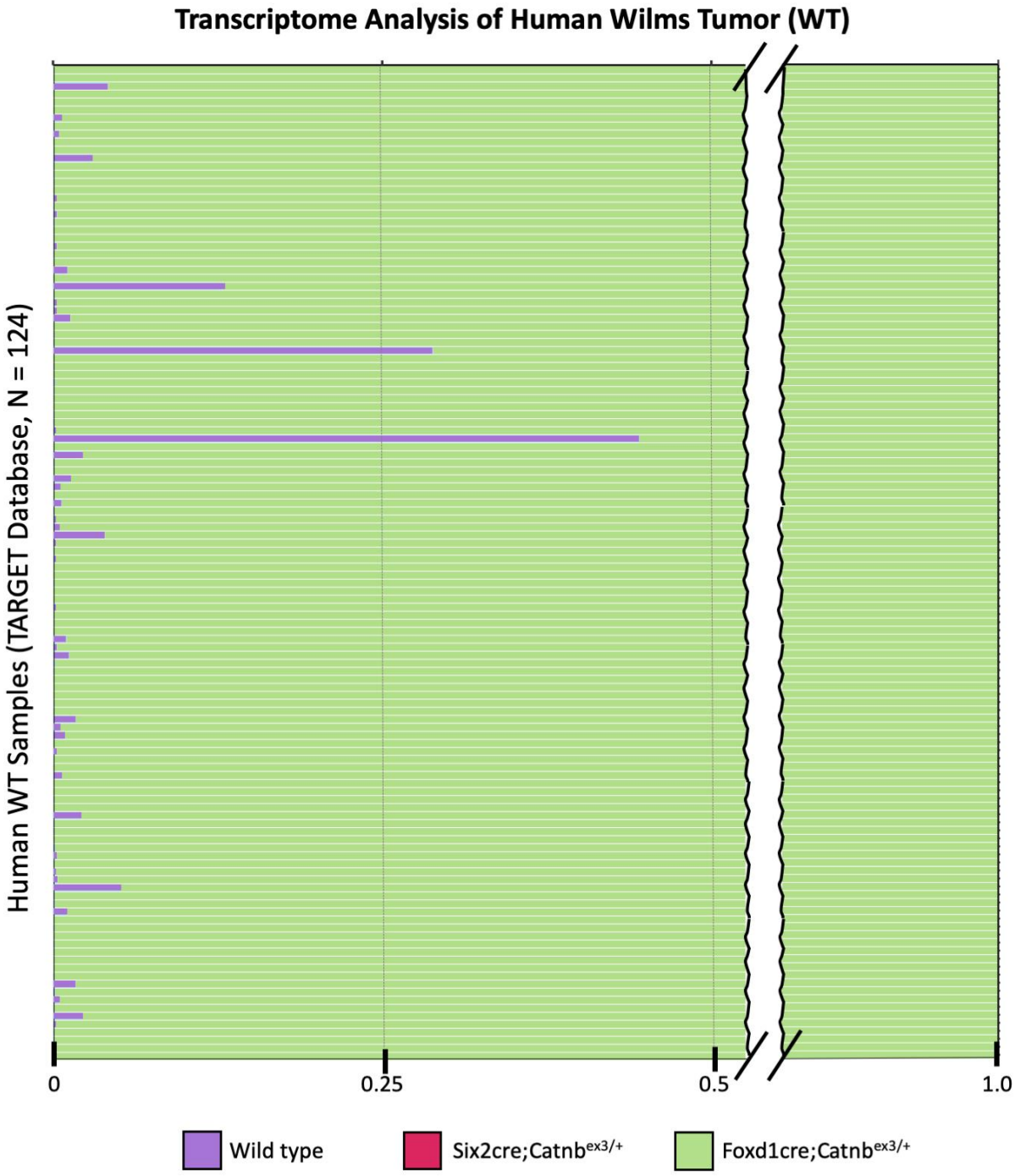

Figure 7. Human Wilms tumor shows molecular characteristics similar to mutant mouse kidneys with activation of beta-catenin in stromal lineage. RNA-seq on E12.5 wild type, Six2cre;Catnb$^{ex3/+}$, and Foxd1cre;Catnb$^{ex3/+}$ mutant kidneys (N = 3 for each genotype) were compared to human Wilms tumor RNA-seq data obtained from the publicly available

TARGET database (N = 124 samples). Using neural network classification, mapping scores ranging from 0 to 1.0 were generated for each human WT sample measuring similarity of expression of the 2806 identified likely direct targets of beta catenin to that of each of the mouse genotypes, with these results showing expression of these genes in the tumor samples was most similar to the Foxd1cre;Catnb$^{ex3/+}$ mouse model (green bars), with few tumors showing a small degree of similarity to wild type kidneys (purple bars), and none of the samples showing any significant degree of similarity to the Six2cre;Catnb$^{ex3/+}$ expression profile.

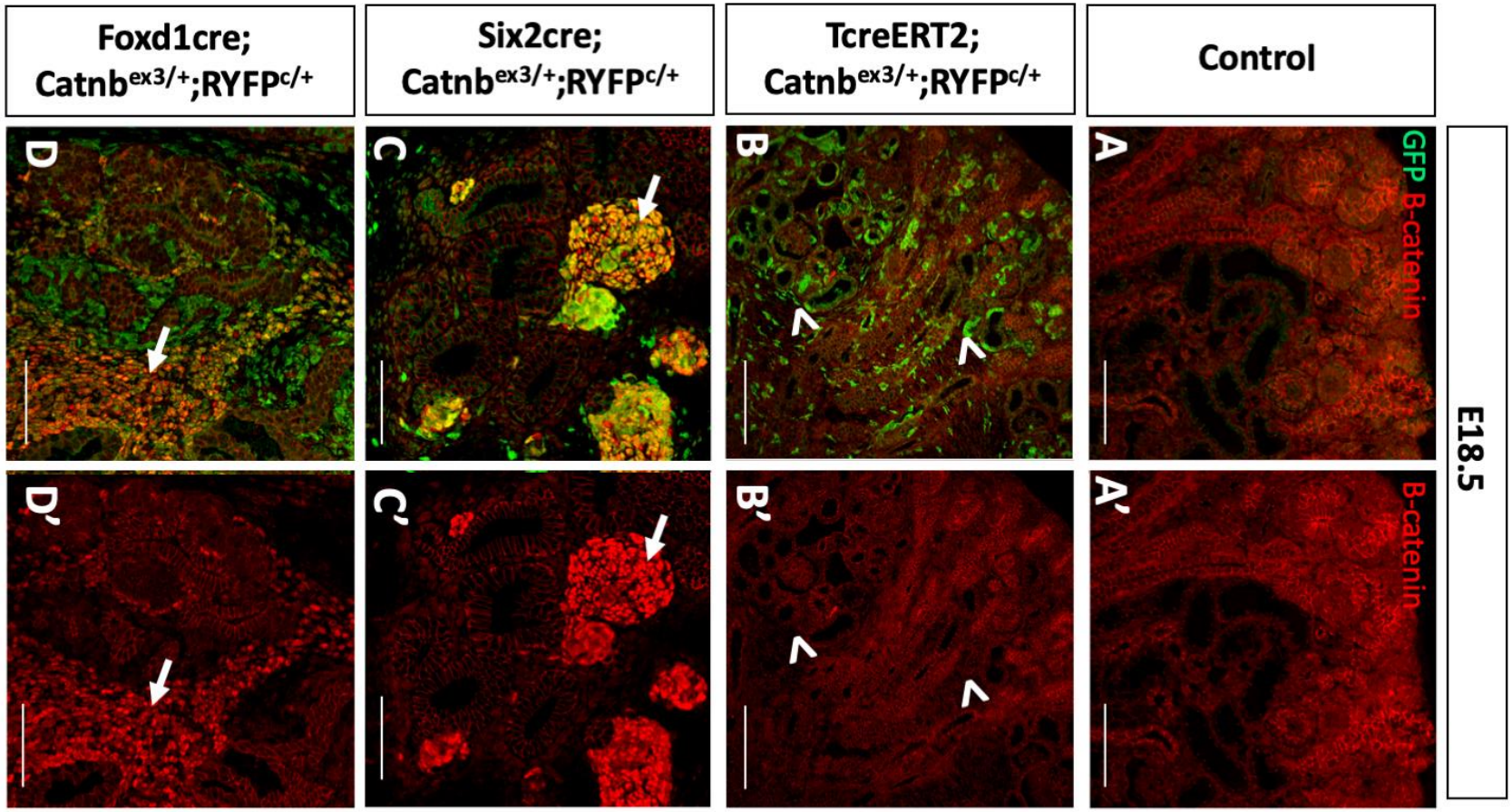
Foxd1cre;
Catnb^ex3/+;RYFP^c/+
Six2cre;
Catnb^ex3/+;RYFP^c/+
TcreERT2;
Catnb^ex3/+;RYFP^c/+
Control
D
C
B
A
GFP B-catenin
D'
C'
B'
A'
B-catenin
E18.5

Figure 8. Beta-catenin activation in early metanephric kidney precursors does not result in nuclear beta-catenin despite evidence of recombination.

TcreERT2;Catnb$^{ex3/+}$;RosaYFP$^{c/+}$ mutants given 2 mg per 40 g body weight of tamoxifen at E9.5 demonstrate recombination by the presence of lineage-traced cells (B, arrowhead); however, these cells unexpectedly lack detectable expression of beta-catenin (B'). Conversely, strong nuclear expression is observed in Six2cre and Foxd1cre mutant kidneys (C, D, arrows). Scale bar = 100 um; N = 3 for each timepoint/genotype.

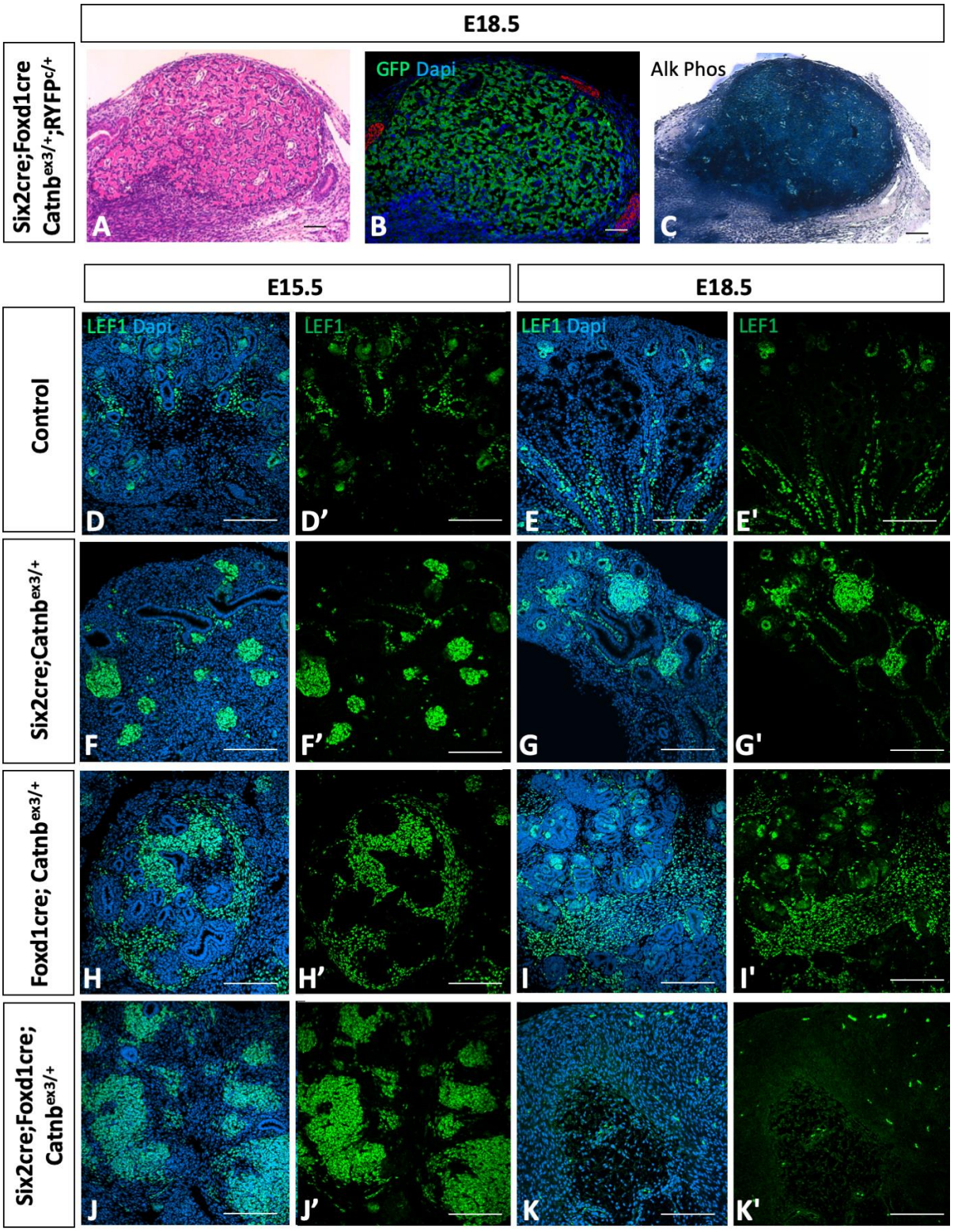

Figure 9. Beta-catenin activation in dual NPC and stromal lineages results in the development of bone. Six2cre;Foxd1cre;Catnb$^{ex3/+}$ mutants kidneys resemble "bone-like" tissue at E18.5 by H&E (A), with reporter expression confirming these cells originated from

the targeted cell populations (B) and demonstrate strong expression of the bone marker alkaline phosphatase (C). While Lef-1, a transcription factor previously shown to interact with beta-catenin to promote osteoblast activity (Hoeppner et al., 2011, Li et al., 2018), is up-regulated in all mutant lines (F-I), the “bone-like” phenotype is only observed in the Six2cre;Foxd1cre;Catnb$^{ex3/+}$ mutants. Scale bar = 100 um; N = 3 for each timepoint/genotype.

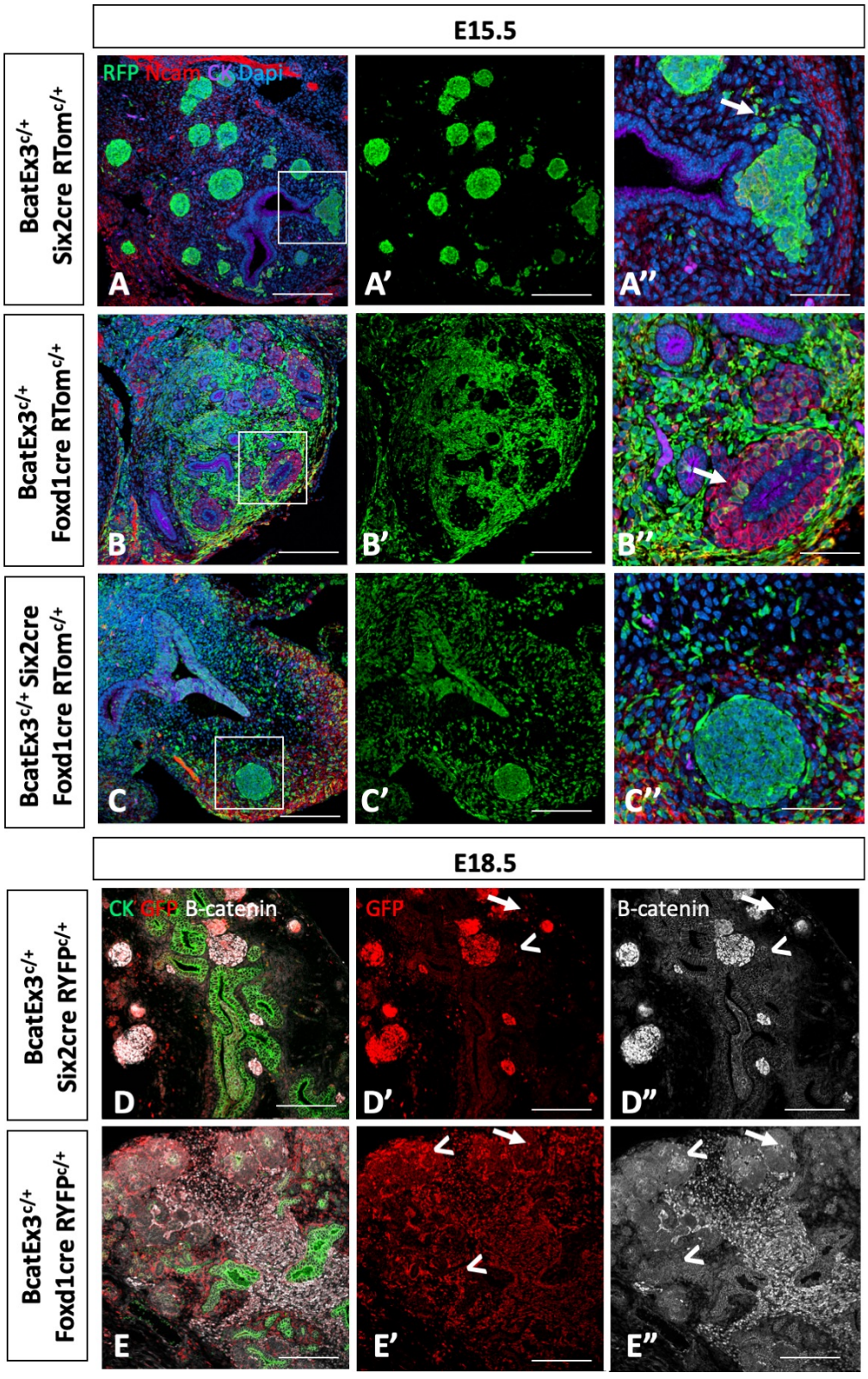

Figure S1. Lineage-tracing of beta-catenin activation in NPC and stromal cells confirm increased expression of nuclear beta-catenin in recombined cells. Use of RosaYFP and RosaRFP reporters in our mutant mouse lines show evidence of recombination in the NPC lineage (A), stromal lineage (B), and dual Six2cre and Foxd1cre mutant kidneys (C). Recombined cells in the Six2cre;Catnb$^{ex3/+}$ mutants are scattered amongst the stroma (A", arrow) with some cells expressing nuclear beta-catenin (D", arrow) while others do not (D", arrowhead). Foxd1cre;Catnb$^{ex3/+}$ mutants also show lineage infidelity, as a few scattered NPCs show evidence of recombination (E') with some cells expressing nuclear-beta-catenin (E", arrow) but others without (E", arrowhead). N = 3 for each timepoint/ genotype.

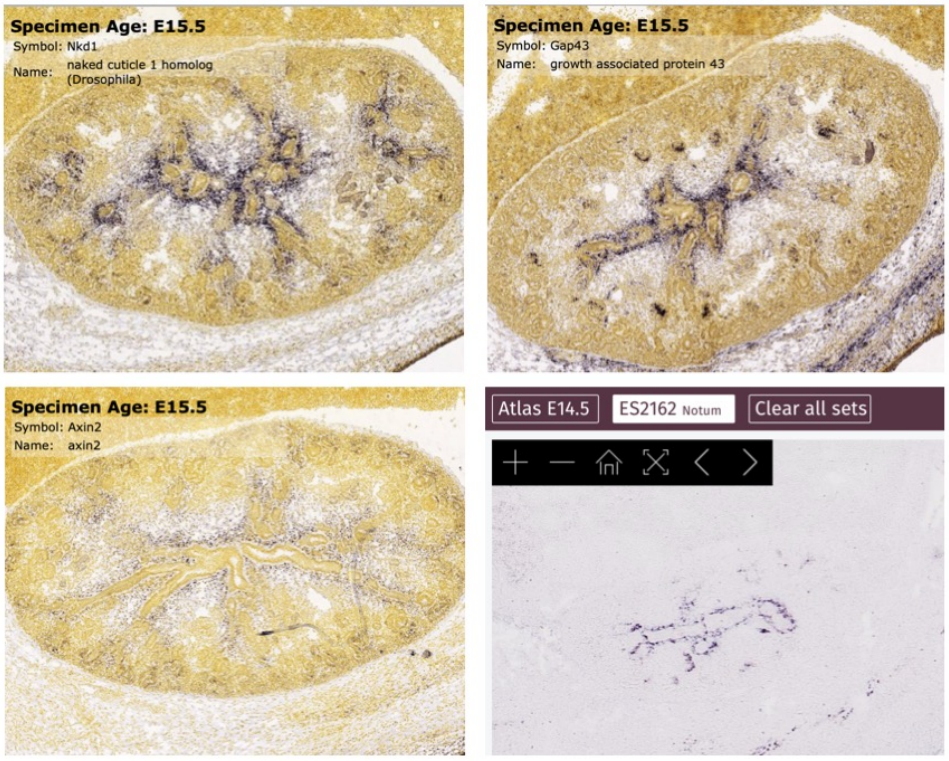

Figure S2. Beta-catenin activation drives the expression of genes normally localized to the developing renal interstitium. In-situ hybridization data from publicly available expression atlas (including Allen Brain Atlas and Genepaint) show stromal expression of Nkd1, Gap43, Axin2, and Notum – all genes also found to be up-regulated in both Six2cre;Catnb$^{ex3/+}$ mutants and Foxd1cre;Catnb$^{ex3/+}$ mutants as well at human WTs with CTNNB1 activating mutations.

Table S1

Click here to Download Table S1

Table S2

Click here to Download Table S2

Table S3

Click here to Download Table S3

Table S4

Click here to Download Table S4

Table S5

Click here to Download Table S5

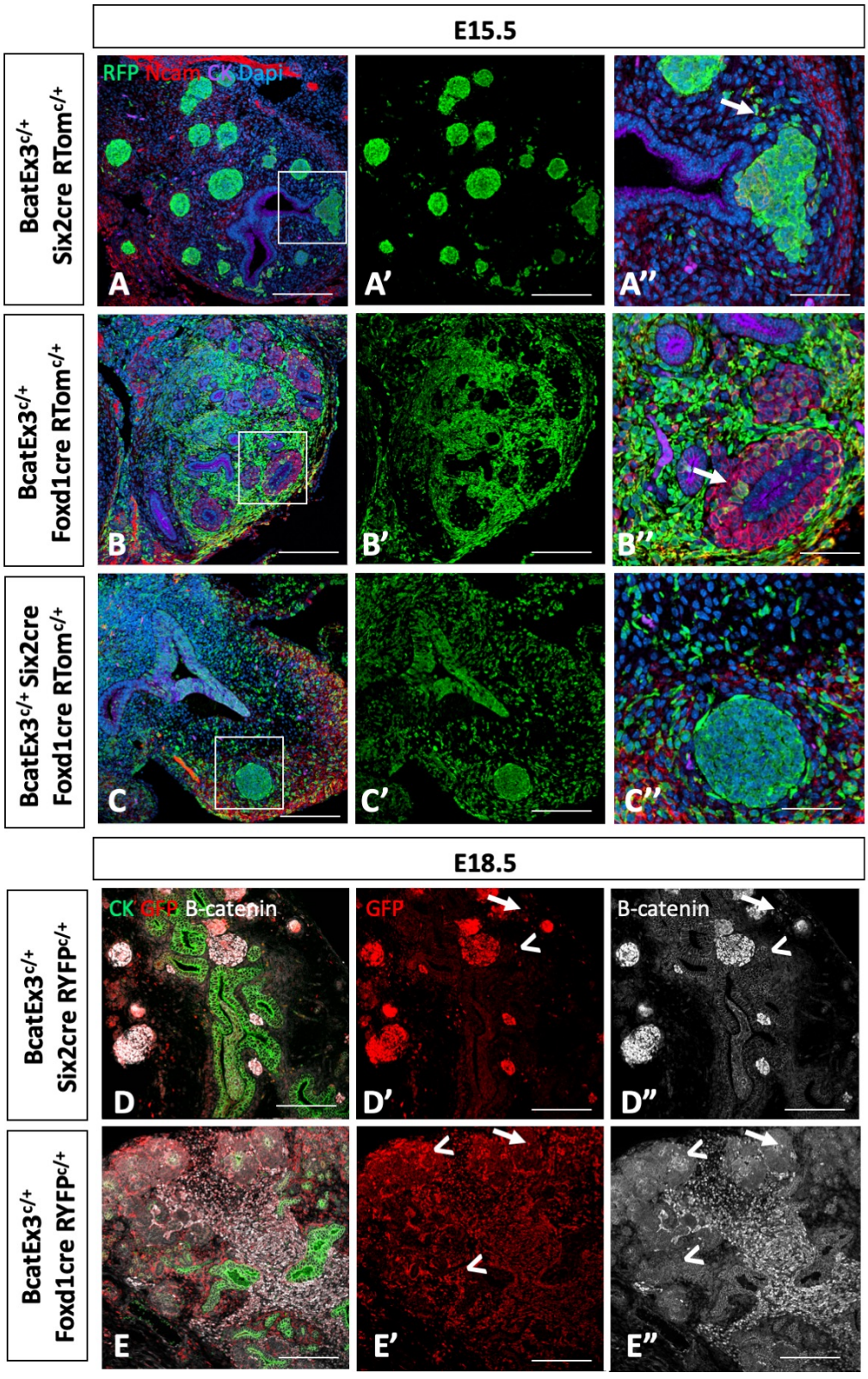

Figure S1. Lineage-tracing of beta-catenin activation in NPC and stromal cells confirm increased expression of nuclear beta-catenin in recombined cells. Use of RosaYFP and RosaRFP reporters in our mutant mouse lines show evidence of recombination in the NPC lineage (A), stromal lineage (B), and dual Six2cre and Foxd1cre mutant kidneys (C). Recombined cells in the Six2cre;Catnb$^{ex3/+}$ mutants are scattered amongst the stroma (A", arrow) with some cells expressing nuclear beta-catenin (D", arrow) while others do not (D", arrowhead). Foxd1cre;Catnb$^{ex3/+}$ mutants also show lineage infidelity, as a few scattered NPCs show evidence of recombination (E') with some cells expressing nuclear-beta-catenin (E", arrow) but others without (E", arrowhead). N = 3 for each timepoint/ genotype.

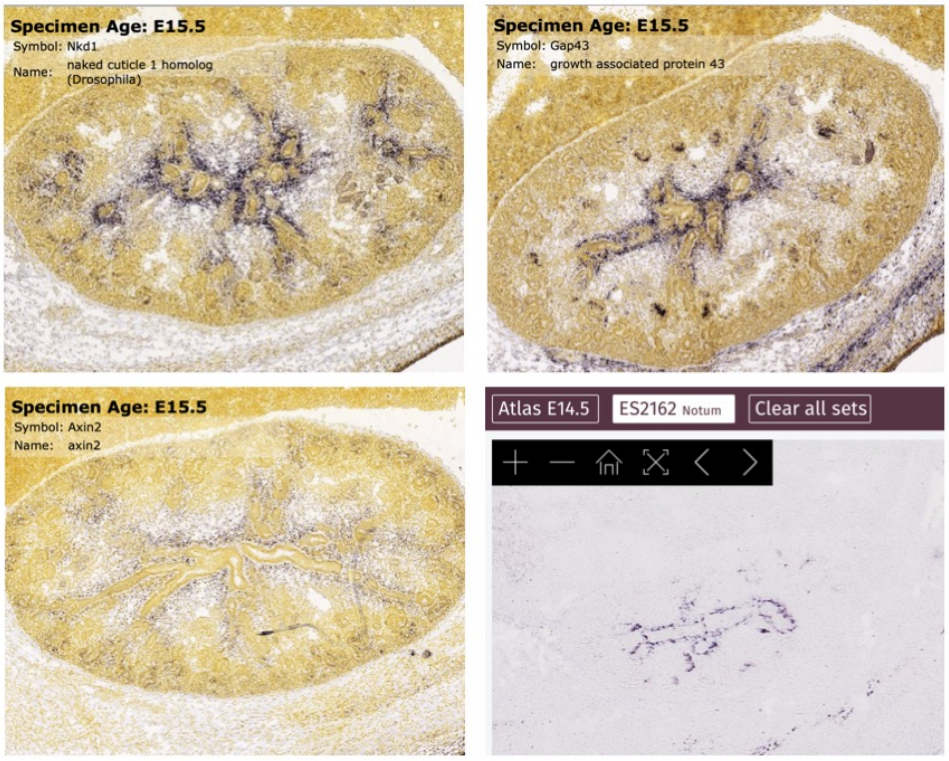

Figure S2. Beta-catenin activation drives the expression of genes normally localized to the developing renal interstitium. In-situ hybridization data from publicly available expression atlas (including Allen Brain Atlas and Genepaint) show stromal expression of Nkd1, Gap43, Axin2, and Notum – all genes also found to be up-regulated in both Six2cre;Catnb$^{ex3/+}$ mutants and Foxd1cre;Catnb$^{ex3/+}$ mutants as well at human WTs with CTNNB1 activating mutations.

Table S1. Differential gene expression from RNA-seq of E12.5 Six2cre;Catnb$^{ex3/+}$ versus Foxd1cre;Catnb$^{ex3/+}$ mutant kidneys

Click here to Download Table S1

Table S2. Direct β-catenin targets identified from RNA-seq of E12.5 Six2cre;Catnb$^{ex3/+}$ and Foxd1cre;Catnb$^{ex3/+}$ mutant kidneys

Click here to Download Table S2

Table S3. Differential gene expression in WT with CTNNB1-activating mutations versus tumors without CTNNB1-activating mutations

Click here to Download Table S3

Table S4. Transcriptome analysis of human WT and mutant mouse models

Click here to Download Table S4

Table S5. Bioinformatic algorithms and software

Click here to Download Table S5